Journal of Chromatography, 149 (1978) 71–91

CHROM. 10,891

MASS TRANSFER PHENOMENA IN GEL PERMEATION CHROMATOGRAPHY

M. E. VAN KREVELD and N. VAN DEN HOED
Koninklijke/Shell Laboratorium, Amsterdam Shell Research B.V., Amsterdam (The Netherlands)

SUMMARY

Very accurate determinations of the first and second moments of sample peaks have been made from measurements at different velocities of the mobile phase. Radial diffusion coefficients of macromolecules in the pores of the column filling material have been obtained from the second moments with the aid of the non-equilibrium theory of chromatography. It has been found that a flow-dependent mass transfer term also plays a role in the exchange between the mobile and stationary phases. Neglecting minor terms, peak broadening in gel permeation chromatography can be considered to be dependent on diffusion and flow-dependent mass transfer.

INTRODUCTION

Nearly every chromatographic technique can be optimized and adapted to new applications if one has a deeper understanding of the underlying physical separation process. In gel permeation chromatography (GPC), the state of the art has not reached this stage yet. The theoretical models that have been proposed to date have tried to explain GPC in terms of separation by steric exclusion[1–3], flow[4–7] or restricted diffusion[8]. There are several reviews[9–11] that give many references and discuss the different theories. Unfortunately, in most publications different mathematical descriptions of the separation mechanism were chosen, depending on the particular phenomenon to be studied. For example, the position of a peak and its broadening are usually derived under conflicting boundary conditions. Also, it must be realized that most of the published experimental work in GPC has insufficient accuracy for the various factors that contribute to the total separation effect to be interpreted satisfactorily. Some workers have not even tried to measure the relevant quantities at all. Often, therefore, one sees observations of maxima positions of asymmetrical peaks that do not permit any conclusions to be drawn about the separation mechanism, because there is no relationship between these positions and any physical parameter.

From the peak broadening, information can be derived about the mechanism by which solutes are exchanged between the mobile phase and the stationary phase. Most workers have drawn final conclusions from a comparison between theoretical assumptions and measured peak broadening values in an obscure way by showing graphs of theoretical and measured HETP values as a function of the mobile phase

velocity. However, as the total HETP is a function of different contributions, which are sometimes either of very different or of the same order of magnitude, it is often unclear into which contribution to the total broadening effect the experiments provide a deeper insight. To resolve this dilemma, we have not taken the agreement between theoretical and experimentally determined HETPs as a final criterion, but have tried to answer the question of which parameters of the physical separation process can be determined from the measurement of peak position and broadening and how accurately this can be done.

A realistic approach will be to choose a theory that is free from the drawbacks of the theories already mentioned. An obvious first choice is the non-equilibrium description of chromatography[12–15]. This is a consistent general theory that is applicable to chromatographic processes, which has the added advantage that assumptions about possible mechanisms can easily be incorporated, either in the physical parameters of the separation mechanism or in the initial and boundary conditions. Therefore, it is worthwhile investigating whether this theory is also able to describe the GPC process satisfactorily.

The theory yields a relationship between the central reduced second moment, μ_2, of a chromatographic peak, the mobile phase velocity and the parameters of some fundamental contributions to the total mass transfer process, such as the inter-particle displacement and the intra-particle transport in the grain, of solutes. In addition, one must recognize that in addition to the column process, the trivial factor of instrumental broadening often plays a considerable role in the total peak broadening. If the aim is to determine one particular parameter out of those which together contribute to the total peak broadening, one has to choose the conditions for the experiments very carefully. Accordingly, in our experiments we varied the conditions over such a range that the ratio of the various contributions to the peak broadening changed considerably, so as to ensure that the different factors could be distinguished from each other. On the other hand, we also bore in mind that, in order to clarify the establishment of equilibrium between the stationary and mobile phases, the system had to be forced considerably from the equilibrium situation for the benefit of the observation.

Under the above experimental conditions, the peaks obtained are skewed. According to the theory[12,13], the significant quantities that contain information about the separation mechanism are the first and second moments of the peaks. It is difficult to measure the second moment of a tailing peak reliably and consequently, before the experiments can be carried out, we must have a clear idea about the requisite accuracy for such measurements to form a basis for meaningful conclusions. To give an idea of the accuracy that has to be achieved before a second moment can be measured, we may recall that particularly with skewed peaks most of the μ_2 value is determined by contributions from the outer wings of the peak very near the baseline, where the signal is already less than 1 % of the peak maximum value[16]. Hence, we made a special effort to achieve the desired accuracy and full details are given under Experimental.

THEORETICAL

The mass balance equation of a solute in a one-dimensional flow system in a chromatographic column packed with spherical particles of diameter R_0 (cm) can be described by a partial differential equation[14,17]:

$$D_p \cdot \frac{\partial^2 c}{\partial x^2} - u \cdot \frac{\partial c}{\partial x} - \frac{\partial c}{\partial t} = Q_c \tag{1}$$

where D_p (cm²/sec) is the coefficient of longitudinal dispersion, c (g/cm³) is the concentration of the solute in the mobile phase, x (cm) is the distance from the beginning of the column, u (cm/sec) is the linear velocity of the mobile phase and t (sec) is time. The rate of change of concentration in the inter-particle space as a consequence of the mass transfer either into or from the pores is denoted by Q_c (g/sec·cm³). The diffusion of a solute into a porous spherical grain is, according to the well known diffusion theories[18], given by another differential equation:

$$D_r\left(\frac{\partial^2 C}{\partial r^2} + \frac{2}{r} \cdot \frac{\partial C}{\partial r}\right) = \frac{\partial C}{\partial t} \tag{2}$$

where D_r (cm²/sec) is the coefficient of diffusion in the particle, C (g/cm³) in the concentration of solute in the porous particle and r (cm) is the radial coordinate within the grain with the origin chosen in the centre of the sphere. A possible third differential equation, describing adsorption on the internal surface of the grains, has not been taken into account because we have no indication that this effect exists in the phase system under consideration, as will be shown under Experimental.

For the simultaneous solution of eqns. 1 and 2, we need an expression for Q_c. Two different relationships can be introduced, depending on the physical model that is chosen. If an immediate equilibrium is established between the concentrations of solute in the mobile phase and in the pore openings, Q_c can be written as[14]

$$Q_c = \frac{3\varphi D_r}{R_0}\left(\frac{\partial C}{\partial r}\right)_{r=R_0} \tag{3}$$

where φ denotes $\beta(1 - \alpha)/\alpha$, in which α is the external porosity in the column and β the internal porosity in the grains. Physically, it can also be assumed that an absorbed thin layer surrounds the grain and gives rise to a particular resistance to mass transport of solutes if they emerge from the pores into the inter-particle space or move in the opposite direction.

If the rate of transfer through this film is assumed to depend linearly on the difference between the actual and the equilibrium concentration[19], then Q_c can be written as

$$Q_c = -H_c(K_c - C_{r=R_0}) \tag{4}$$

where H_c is a mass transfer coefficient (1/sec), $C_{r=R_0}$ is the concentration at the opening of the pore where $r = R_0$ and K_c is the equilibrium constant.

From eqns. 1 and 2, a relationship can be derived via Laplace transformation[12–14] between the length of the column, L, the first reduced moment, μ_1', the second reduced central moment, μ_2, of the chromatographic peak and the parameters used in eqns. 1 and 2. Two different equations can be derived if we assume either immediate

equilibrium at the pore openings or the existence of a film resistance round about the grain. In the first instance[15] we obtain

$$L \cdot \frac{\mu_2}{(\mu_1')^2} = \frac{2D_p}{u} + \frac{2u\varphi K_c}{(1+\varphi K_c)^2} \cdot \frac{R_0^2}{15D_r} \tag{5}$$

and in the second

$$L \cdot \frac{\mu_2}{(\mu_1')^2} = \frac{2D_p}{u} + \frac{2u\varphi K_c}{(1+\varphi K_c)^2}\left(\frac{R_0^2}{15D_r} + \frac{\varphi}{H_c}\right) \tag{6}$$

In order to decide whether eqns. 5 and 6 are significantly different, we estimated the order of magnitude of the factor φ/H_c. This can be calculated if we assume that the transport through a surrounding thin absorbed film of mobile phase is governed by diffusion. In our experiments we used grains with $R_0 = 6.25 \cdot 10^{-3}$ cm and an internal porosity of about 0.6. Straightforward calculation gives a pore opening area of about 300 cm^2 per cubic centimetre of column. The rate of influx of the solute into the mobile phase, which is equal to the rate of decay from the pores, per unit volume can be written either as $Q_c = D_r \cdot$(pore area/cm^3 column)$\cdot (\partial c/\partial r)$ or as $Q_c = H_c \Delta c = H_c \cdot (\partial c/\partial r) \cdot \Delta r$. Combination yields

$$H_c = \frac{300\, D_r}{\Delta r} \tag{7}$$

Even if we assume that the layer thickness, Δr, has an unrealistically large value of about 1000 Å, the factor φ/H_c in eqn. 6 can be neglected compared with $R_0^2/15D_r$ and we can confine ourselves to the use of eqn. 5.

Kubín[20] also derived a similar equation for the GPC mechanism:

$$L \cdot \frac{\mu_2}{(\mu_1')^2} = \frac{2D_p}{u} + \frac{2u\varphi K_c(1-\varrho^3)}{[1+\varphi K_c(1-\varrho^3)]^2} \cdot [1 - G(\varrho)] \cdot \frac{R_0^2}{15D_r} \tag{8}$$

where $\varrho = R/R_0$ and R is the radius of the grain centre that is supposed to be impermeable to the solute macromolecules of a certain size. This assumption will be discussed later. The function $G(\varrho)$ is as defined by Kubín[20]. We calculated the factor $1 - G(\varrho)$ for the different macromolecules used in our investigation, but its value was always about 1 and changed by only a few percent on going from small to large molecules. This difference is far below the accuracy of $L \cdot \mu_2/(\mu_1')^2$ that we could achieve in our experiments. According to Kubín[20], the factor $1 - \varrho^3$ has a restricted diffusion character where he suggests ϱ will be dependent on flow-rate; then one expects the peak positions as a function of elution volume to change if the mobile phase velocity is increased, because $1 - \varrho^3$ is also a factor in his expression for μ_1':

$$\mu_1' = \frac{L}{u}[1 + \varphi K_c(1-\varrho^3)] \tag{9}$$

Now we can rewrite μ_1 as a function of elution volume by multiplying by the volume flow, v (cm³/sec):

$$\mu'_{1v} = \frac{Lv}{u}[1 + \varphi K_c(1 - \varrho^3)] = V_0[1 + \varphi K_c(1 - \varrho^3)] \tag{10}$$

where V_0 is the inter-particle volume of the column. Even with the experimental accuracy that we could attain, we found no evidence for the existence of this factor; the μ'_{1v} of four different polystyrene molecules remained constant up to very high velocities (see, *e.g.*, Fig. 1). In fact, over the whole range of flow velocities we found the same value of φK_c as could theoretically be calculated by assuming that all molecules penetrate into the whole particle up to the centre. This has already been shown in our previous work[21] and was corroborated by the results of our new experiments. In addition, the value of the factor $1 - \varrho^3$ will not be very different from 1 and can therefore be neglected. In consequence, we have only to deal with an equation similar to eqn. 5.

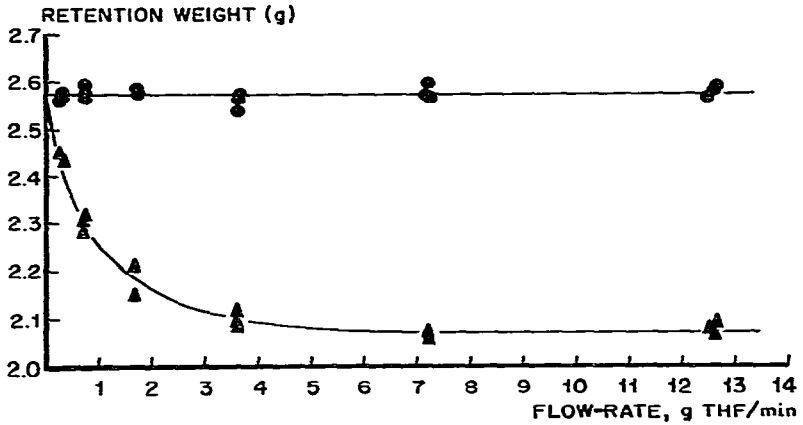

Fig. 1. Influence of flow-rate on the position of peak maximum and first statistical moment of polystyrene 51 000. Early-stage column; Variscan detector. ●, First moment; ▲, peak maximum.

Let us consider more closely the possible flow patterns that can originate in a pore opening at the surface of the grain as the mobile phase flows past. There is some evidence, also from some preliminary experiments of our own, that the mobile phase liquid will be adsorbed, and hence immobilized, on the polar SiO_2 surface of the silica gel. However, the effect is probably restricted to one or two layers of molecules. This is only a few percent of the average pore radius in Porasil C. The remaining part of the pore diameter is filled with liquid that will still be completely mobile, so there is no reason to assume that there is a sudden sharp boundary between the liquid flowing alongside the grain and the stagnant liquid within the pores. One can imagine that eddies will be produced to a certain depth in the pores by the shear of mobile phase that flows along the outside. In that event the factor D_r in eqn. 2 must be regarded as a coefficient of effective mass transport in the pore (denoted by $D_{r\,eff}$). With the above assumptions, this effective transport coefficient will consist

of two contributions; one is hindered diffusion proper in the pores, D_r, and the other part will be due to eddies with a coefficient D^1, resulting in

$$D_{r\,\mathrm{eff}} = D_r + uD^1 \tag{11}$$

With this substitution, we again solve eqns. 1 and 2 via Laplace transformation and instead of eqn. 5 we now obtain the equation

$$L \cdot \frac{\mu_2}{(\mu_1')^2} = \frac{2D_p}{u} + \frac{2u\varphi K_c}{(1+\varphi K_c)^2} \cdot \frac{R_0^2}{15(D_r + D^1 u)} \tag{12}$$

In all of the equations mentioned, D_p can be written[15] as $D_m + Au$, giving for the last equation

$$L \cdot \frac{\mu_2}{(\mu_1')^2} = 2A + \frac{2D_m}{u} + \frac{2u\varphi K_c}{(1+\varphi K_c)^2} \cdot \frac{R_0^2}{15(D_r + D^1 u)} \tag{13}$$

where D_m is the well known molecular diffusion coefficient and A is the spreading coefficient due to uneven flow effects in the mobile phase.

EXPERIMENTAL

Apparatus

The chromatographic equipment is shown in Fig. 2. The system consists of the following components: (a) combined storage vessel and degassing unit, stainless steel, Koninklijke/Shell Laboratorium (Amsterdam) design; (b) membrane pump, double-headed; Orlita DMP 1515; (c) pulsation damping device; home-made; (d) pressure transducer; Tyco Bytrex Div.; (e) sample introduction system; Model U6K, Waters Assoc.; (f) chromatographic column, stainless steel, length 41.0 cm, I.D. 0.39 cm, packed with Porasil C; (g) ultraviolet absorption detector; two different types were used, first a Varian Aerograph Variscan variable-wavelength detector operating at 261 nm, and later a Waters Model 440 fixed-wavelength detector working at 254 nm; (h) double-pen flat-bed strip-chart recorder; Servogor RE5; (i) electronic balance; Mettler PE 162; (j) balance control unit; Mettler BE 11; (k) *X–Y* recorder; Hewlett-Packard 3480 B; (m) keyboard; Koninklijke/Shell Laboratorium (Amsterdam) design; (n) two-channel data logger, sample frequencies ranging from 0.01 to 50 Hz to be chosen in 12 different steps; Koninklijke/Shell Laboratorium (Amsterdam) design; (o) digital cassette recorder; maximum recording rate 300 characters per second; Koninklijke/Shell Laboratorium (Amsterdam) design.

The mobile phase leaving the detector is collected in a vessel that is continuously weighed on the electronic balance. The balance and the detector signals are recorded alternately on the same tape, so that the detector signal and the associated amount of mobile phase eluted are stored in pairs. In each experiment 500–1000 paired balance and detector data were measured. The start of the recording is triggered by the pulse of a microswitch connected to the sample introduction system. In this arrangement the influence of flow variation within one chromatographic experi-

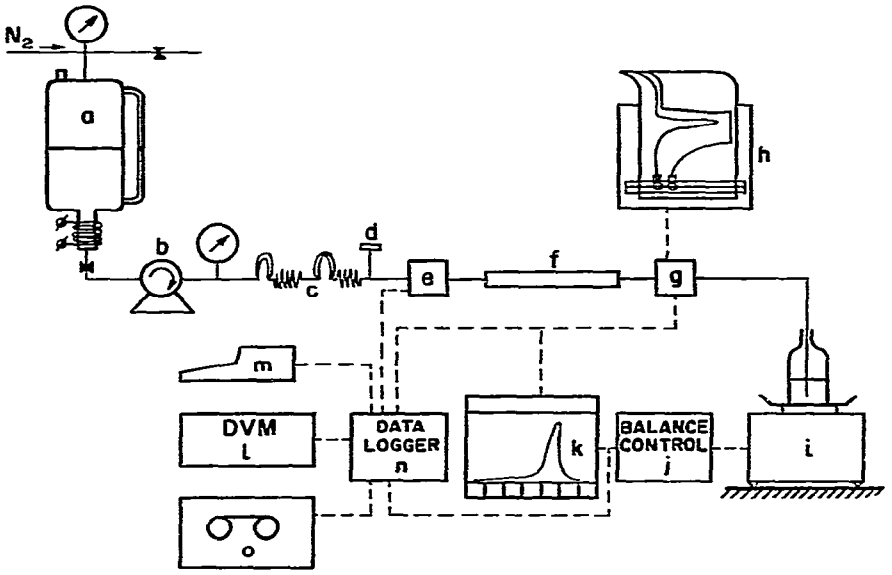

Fig. 2. Experimental arrangement. Dotted lines indicate electrical connections; for explanation, see text.

ment on the measured retention volume and retention volume distribution is considerably smaller than in classical retention time measurements.

Chromatographic system

Tetrahydrofuran (THF) distilled and stored under a nitrogen atmosphere with 25 ppm of Ionol® as antioxidant was used as the mobile phase. The solutes used consisted of toluene and standard polystyrenes with specifications given earlier[21] and were prepared as 0.5% solutions in THF. The sample size of the injected solution was chosen such as to make the Waters detector output range from 0.1 to 0.2 absorption unit (AU).

Porasil C, 100–150 mesh, batch 143*, pore volume 0.789 ml/g measured by titration (for procedure see refs. 22 and 23) from Waters Assoc. was used as the stationary phase. The column was prepared according to the dry filling technique described earlier[24]. As stability mattered more than high efficiency in this investigation, vigorous beating was applied in order to obtain a stable packing. A maximum of 2.52 g of Porasil C could be introduced. The plate number of this column was 250 for a toluene sample measured with a flow velocity of 1 ml/min. The results in Table I and Fig. 1 were obtained with a slightly different and less stable column in the early stage of our investigation.

As in our previous study[21], we checked the relationship between column parameters and chromatographic behaviour and found that the total pore volume of the column deviated by less than 2% from the difference in retention volume

* Previous work[21] was carried out with batch 115.

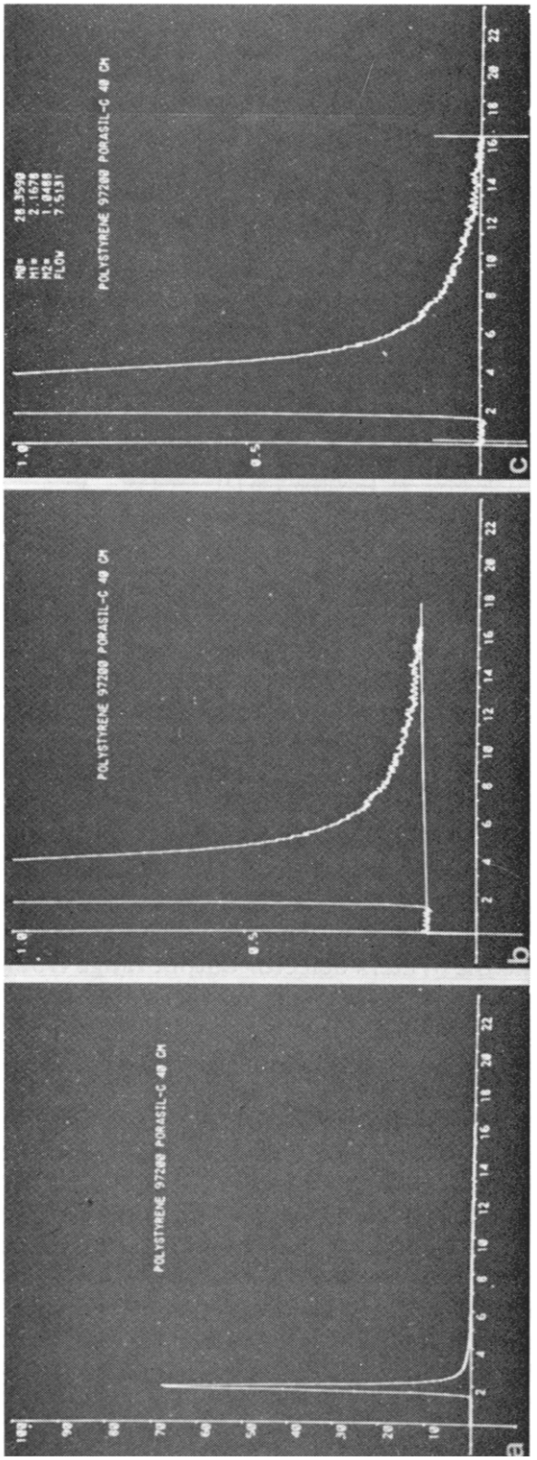

Fig. 3. Determination of statistical moments using a graphic display. (a) Plot of the digitized data of the elution profile, detector signal (mV) *versus* grams of mobile phase. (b) Enlargement (100×) of the lower part with a hypothetical baseline. (c) Baseline-corrected picture with accompanying moment values; vertical bars indicate chosen integration limits.

between solutes totally excluded from the pores and non-excluded solutes. Therefore, absorption of solutes on the internal grain surface could not be demonstrated.

The hold-up of the sample introduction and the detection system was measured by directly connecting these two devices. The retention volume of toluene thus measured was 0.11 g (0.13 cm^3) of mobile phase. All measured first moments were corrected for this blank value.

The instrumental contribution to band broadening ranged from 0.002 to 0.006 g^2 when the velocity was changed from 1 to 12 g/min with toluene as a test substance. This value was neglected in view of the much higher values of the second moments (0.2 to 2.0 g^2) measured with the column installed.

The short-term noise (STN, 1–1000 Hz) of the Waters detector was less than $5 \cdot 10^{-5}$ AU, corresponding to 0.03% of the maximum value of the signals of the solute peaks (*cf.*, Fig. 3). The long-term noise (LTN, drift, ripple, 0.001–1 Hz) amounted to 10^{-4} AU per 1000 sec. STN and LTN values of the Variscan detector are about ten times larger. In experiments with the latter device, the sample concentration had to be chosen such that a signal in the 1–2 AU range was generated, which yielded the same signal-to-noise ratio as in the runs with the Waters detector.

Application software

Two different approaches in software were developed. One design (the batch mode) makes use of straightforward algorithms in which uniform conditions are set. The baseline is assumed to be a straight line through the averages of the first and the last 19 recorded data points. Integration limits are set at 0.02% of the value of the maximum signal and a nine-point quadratic smoothing routine[25] is applied.

In the other approach (the display mode), an interactive procedure was developed using a software package in combination with a graphic terminal. After visual presentation of the enlarged lower portion of the elution profile, the investigator can draw baselines of any desired shape and indicate the integration limits on the basis of the visual representation. The numerical values of the coordinates belonging to the chosen baseline and integration limits are read by the graphic display control and used in the computation routines. Also, the operator can decide whether or not smoothing has to be applied. As a result, a baseline-corrected elution profile (smoothed, if necessary) is replotted on the screen together with the values of the calculated statistical moments (*cf.*, Fig. 3).

The following equations were used in both the batch and interactive procedures:

Zeroth moment:

$$\mu_0 = \sum_{i=f}^{t} y_i \, \Delta x_i \qquad (\text{mV} \cdot \text{g})$$

(Reduced) first moment:

$$\mu_1' = \frac{\sum_{i=f}^{t} y_i x_i \, \Delta x_i}{\mu_0} \qquad (\text{g})$$

(Central reduced) second moment:

$$\mu_2 = \frac{\sum_{i=f}^{t} y_i(x_i - \mu_1')^2 \Delta x_i}{\mu_0} \quad (g^2)$$

Mass flow:

$$F = \frac{x_t - x_f}{(t-f)\Delta\tau} \quad (g/min)$$

where f and t are the indices of the front and the tail limits of integration, y is the baseline-corrected detector signal (mV), x is the amount (g) of mobile phase eluted since the sample was introduced and $\Delta\tau$ is the time interval (min) between two consecutive x-recordings.

The mass flow, F, can be converted into the more general mean linear velocity, $\bar{u}$, by

$$\bar{u} = \frac{FL}{60V_0\varrho} \text{ (cm/sec)}$$

where L is the column length (cm), ϱ is the density of the mobile phase (g/cm^3) and V_0 is the amount of mobile phase (cm^3) between the grains of the stationary phase inside the column, which is set equal to the retention volume of the totally excluded solute PS 411 000[21].

Development of the measuring method

Most of the elution curves produced show extreme tailing. The asymmetry of these profiles is similar to that of the synthetic type I and II profiles of Chesler and Cram[16] (*cf.*, Fig. 4). The measurement of the lower moments (μ_0 and μ_1) of these profiles can be carried out with sufficient accuracy by the batch-mode software package. We determined the standard deviation, S, of ten μ_1 measurements ($S_{\mu_1} < 1\%$ nine degrees of freedom). However, this procedure was found to be of insufficient accuracy when used to determine the second moments of the tailing profiles ($S_{\mu_2} \approx 13\%$, nine degrees of freedom).

For a typical case (PS 51 000 at 4 ml/min), ten chromatographic recordings were collected and evaluated in the batch mode with different settings of the integration limits. The results for μ_2 are given in Table I. It can be seen that μ_2 has a limiting value of about 1.3 g^2, which is obtained when the limits are chosen as low as 0.02%. However under these conditions the spreading in the μ_2 values is dramatic.

According to Chesler and Cram[16], the μ_2 value obtained with integration limits at 0.02% for these types of profile will be about 4% too small, whereas a random noise of 0.1% should be attended with a maximum scatter in μ_2 values of 1%. The latter seems to contradict our findings ($S_{\mu_2} \approx 13\%$). This discrepancy can be attributed to the LTN, which is certainly not random within the period of a single chromatographic experiment. The unpredictable divergent paths of the LTN are inadequately described by a straight baseline estimation as applied in the batch software procedure. As μ_2 is extremely sensitive to small baseline shifts (as will be shown below),

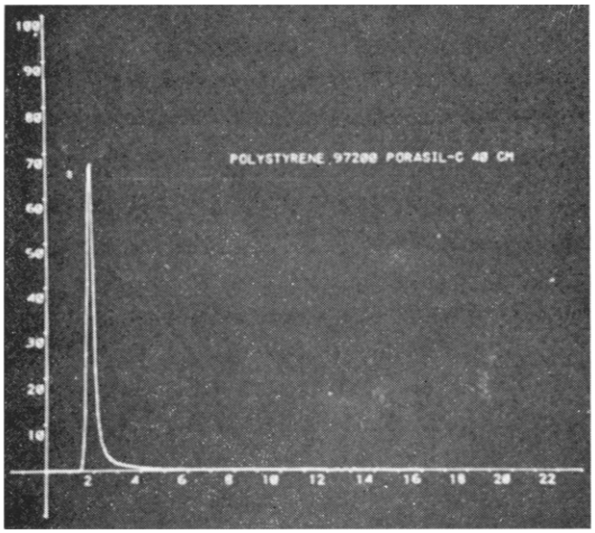

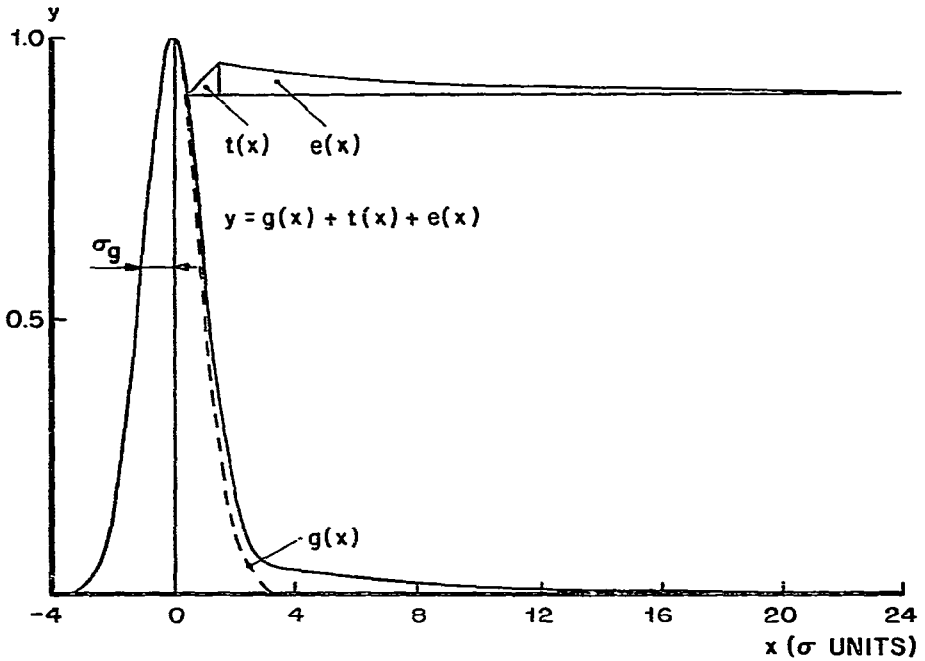

Fig. 4. Comparison between polystyrene 97 200 at a THF flow-rate of 7.5 g/min and a synthetic type I Chesler and Cram profile.

it is understandable that the procedure mentioned will lead to a wide scatter of μ_2 values.

Calculations performed on the synthetic profiles from Chesler and Cram[16] assuming different baselines parallel to the abscissa with limits introduced at 0.01% showed that shifts of only 0.1% yield deviations of 58 and 17% from the exact value of μ_2 for types I (*cf.*, Fig. 5) and II, respectively.

TABLE I

VALUES OF μ_2 FOR POLYSTYRENE 51 000 WITH DIFFERENT INTEGRATION LIMITS

Variscan detector; early-stage column; flow velocity 4 ml/min; batch-mode processing.

	Second moments (g^2)					
	Limit (% of peak maximum)					
	0.75	*0.2*	*0.12*	*0.06*	*0.03*	*0.02*
	0.5831	0.8234	0.9811	1.144	1.264	1.461
	0.5891	0.8124	0.9934	1.089	1.191	1.171
	0.5843	0.8296	0.9923	1.193	1.316	1.391
	0.5850	0.8356	1.004	1.152	1.200	1.278
	0.5831	0.8146	0.9703	1.123	1.310	1.483
	0.5849	0.8113	0.9485	1.092	1.195	1.224
	0.5779	0.8093	0.9322	1.040	1.048	0.9546
	0.5927	0.8433	1.039	1.123	1.159	1.143
	0.5861	0.8451	0.9947	1.169	1.293	1.336
	0.5841	0.8338	0.9959	1.128	1.279	1.344
Mean (g^2)	0.5850	0.8259	0.9851	1.125	1.226	1.279
S_r* (%)	0.67	1.63	3.01	3.91	6.85	12.6
S_{RM}** (%)	0.21	0.52	0.95	1.24	2.12	3.99

* Relative standard deviation.

** Relative standard deviation of the average μ_2.

Baseline shifts on an actual chromatogram of PS 97 200 were also carried out using the graphic display. Three different baselines were drawn according to the top, average and bottom values of the STN (see Fig. 6). The measured differences in μ_2 ($\pm 17\%$) were of the same order of magnitude as those found for the synthetic profiles. Evidently, both the accuracy and the repeatability attainable in determinations of second moments of tailing profiles are extremely sensitive to the assumptions underlying the baseline estimation. A possible remedy may be to develop elaborate and sophisticated software in order to obtain reliable baseline estimations for all shapes of LTN that can possibly occur. Another, more elegant solution, circumventing the extensive software development, is to draw the most probable baseline directly into a chromatogram displayed on a screen. In this fashion the knowledge of an experienced chromatographer is incorporated more readily into calculations than by first trying to translate it into a software package and subsequently utilizing it in the estimation of the baseline. The display mode, discussed under *Application software*, was checked by a ten-fold experiment using PS 51 000 (flow velocity 4 ml/min). The integration limits were set at points where the assumed baseline coincides with the elution profile (In the same way as the limits in Figs. 7a and b are chosen). This resulted in a distinct reduction of the scatterin the μ_2 values ($S_{\mu_2} = 5.7\%$, nine degrees of freedom).

By comparison, the scatter due to personal interpretation of the chromatograms was of minor importance. The maximal difference between the results of four experienced persons evaluating the same chromatogram was about 1%.

Apart from the effect of baseline estimation, we also examined the influence of digital smoothing on STN, peak shape and calculated moments using the display. The resultant graphs are shown in Fig. 7. It can be seen that the applied nine-point quadratic smoothing filter[25] reduces the standard deviation of the STN by about a factor of two and hardly influences the peak shape, thus confirming the results of

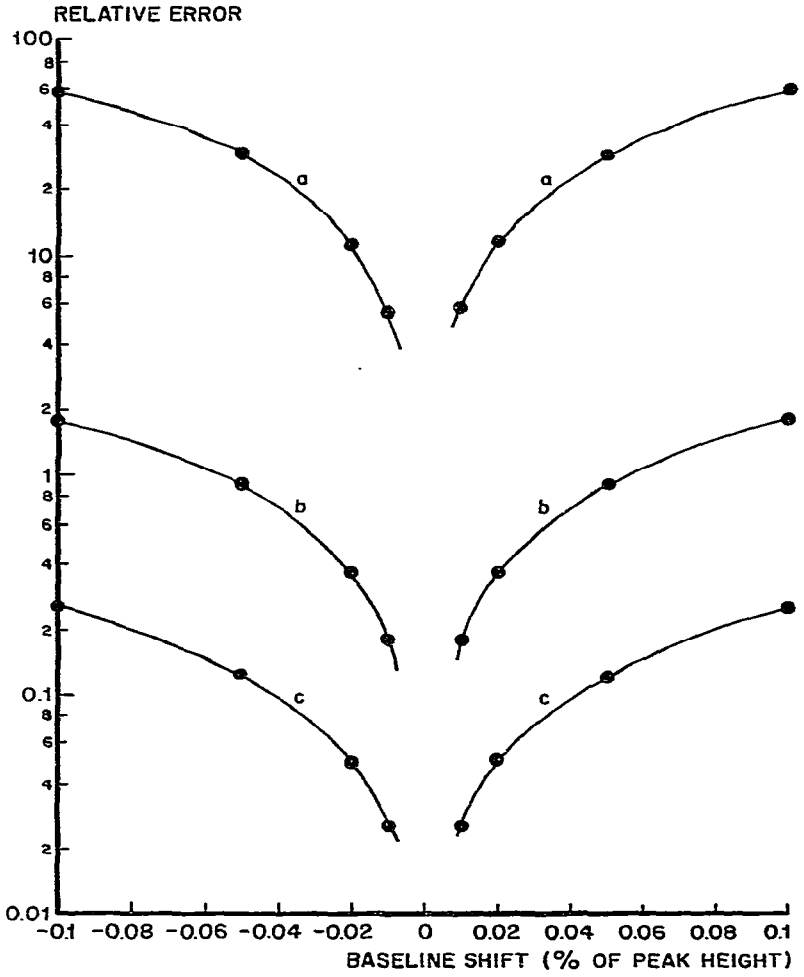

Fig. 5. Influence of baseline shift on the error in the statistical moments for a type I Chesler and Cram profile (integration limits at 0.01% of peak maximum value). $a = \left|\frac{\mu_2 - \tilde{\mu}_2}{\tilde{\mu}_2} \cdot 100\right|$; $b = \left|\frac{\mu_0 - \tilde{\mu}_0}{\tilde{\mu}_0} \cdot 100\right|$; $c = \left|\frac{\mu_1' - \tilde{\mu}_1'}{\sigma_g}\right|$. σ_g is the standard deviation of the Gaussian portion of the profile; the sign (~) denotes the exact value.

Baan[26] for both synthetic and experimental data. The effect of the smoothed STN upon the calculated moments is very small, in agreement with what Chesler and co-workers[16,27] found for the synthetic type I and II profiles. Although the application of digital smoothing has no significant influence on the results of our calculation procedure, we maintained it because it slightly facilitated finding the most probable baselines.

RESULTS

The method of display evaluation of chromatograms was applied to a series of different solutes at various flow velocities. The results are given in Table II together

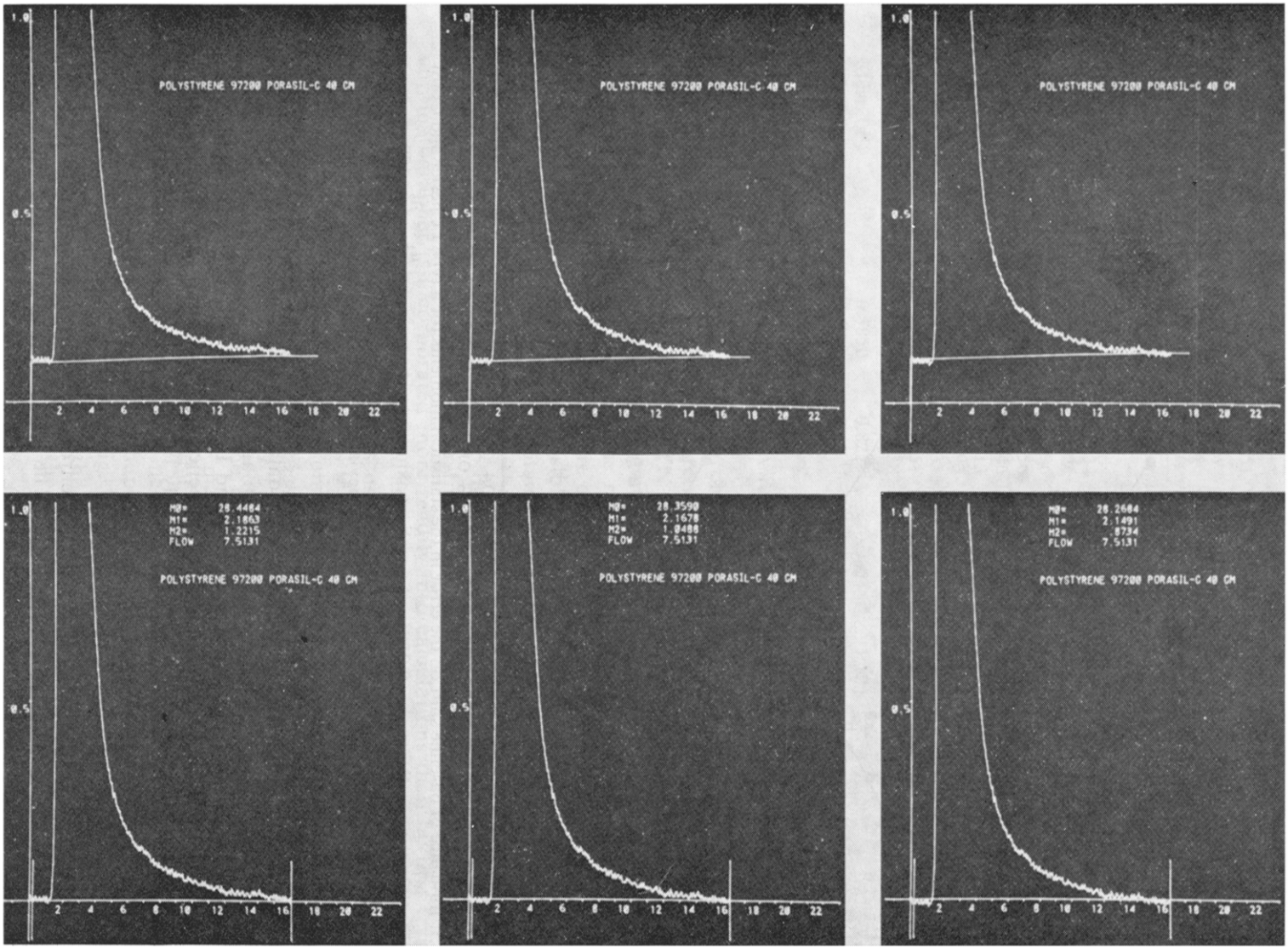

Fig. 6. Influence of baseline estimation on the statistical moments of a tailing elution profile. Detector signal (mV) *versus* eluted mobile phase (g); peak value of the total signal is 70 mV.

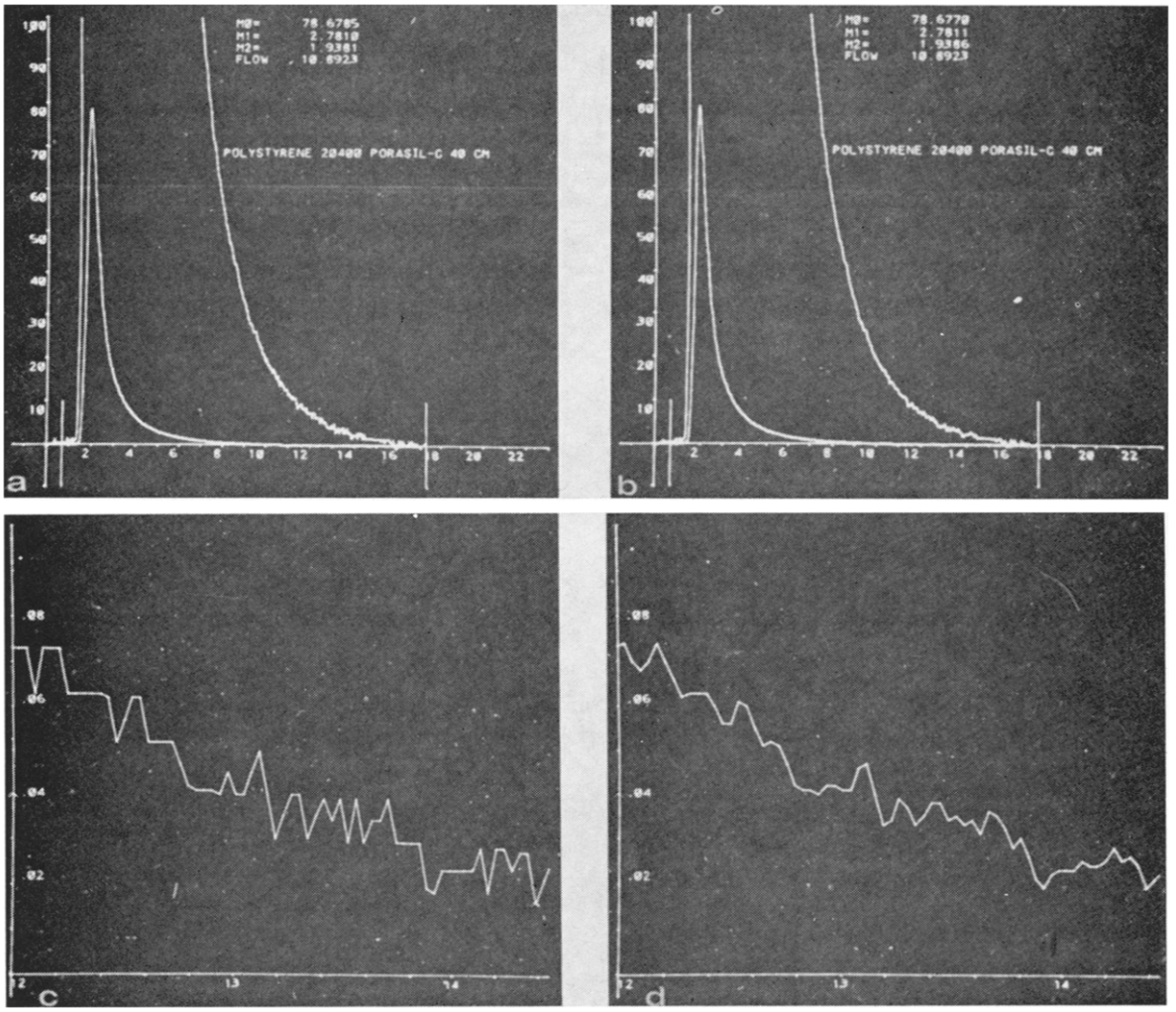

Fig. 7. Influence of digital smoothing on noise, peak shape and moments. Nine-point quadratic smoothing[25]. a and c, raw data; b and d, smoothed data; c and d, partial enlargements of a and b. The vertical scale in a and b applies to the total elution profile; for the enlarged profiles the scale has to be divided by 100.

with the values of $L \cdot \mu_2 - (\mu_1)^2$, being the dependent variable of the eqns. 5 and 13. Before we can test the applicability of these equations, we need to know the values of the parameter $2\eta K_c - 15(1 - \eta K_c)^2 \cdot R_0^2$ for the different solutes. The product ηK_c can easily be calculated from Table II, because it represents the ratio of the accessible part of the pore volume to the amount of liquid outside the grains in the column. As the μ_1' values in Table II have been corrected for the extra-column contributions, we can, using our earlier conceptions[21], determine the factor ηK_c by

$$\eta K_c = \frac{\mu_1'(i) - \mu_1'(\text{PS } 411\,000)}{\mu_1'(\text{PS } 411\,000)}$$

TABLE II

VALUES OF μ_1', μ_2 AND $[L \cdot \mu_2/(\mu_1')^2]$ FOR DIFFERENT SOLUTES AT DIFFERENT FLOW-RATES

Waters detector; display evaluation.

Solute	*Flow-rate (g/min)*	*Flow-rate (cm/sec)*	μ_1'* (g)	μ_2 (g^2)	$[L \cdot \mu_2/(\mu_1')^2]$** (cm)
PS 411 000	0.6273	0.2506	1.7107	0.0246	0.3446
PS 160 000	0.9490	0.3791	1.8944	0.1963	2.2491
	1.9479	0.7781	1.8947	0.3026	3.4671
	3.8799	1.5498	1.8801	0.3484	3.9919
	5.6708	2.2652	1.8827	0.3880	4.4456
	7.4342	2.9696	1.8837	0.4001	4.5842
	10.1676	4.0614	1.8952	0.4344	4.9772
	11.5236	4.6031	1.9108	0.4459	5.1090
PS 97 200	0.9042	0.3612	2.0480	0.2542	2.5235
	1.9485	0.7783	2.0350	0.4500	4.4673
	1.9413	0.7755	2.0392	0.4536	4.5031
	3.8500	1.5379	2.0243	0.5652	5.6110
	5.6397	2.2528	2.0173	0.6138	6.0934
	7.5131	3.0011	2.0243	0.7404	7.3502
	8.9879	3.5902	2.0330	0.7786	7.7295
	10.1221	4.0433	2.0368	0.7941	7.8833
PS 51 000	0.8732	0.3488	2.1630	0.2454	2.0684
	1.8120	0.7238	2.2025	0.4424	3.7288
	3.6022	1.4389	2.1974	0.7473	6.2987
	5.3434	2.1344	2.1971	1.0285	8.6689
	7.0113	2.8007	2.2331	1.4816	12.4879
	9.6145	3.8405	2.2189	1.5682	13.2178
	10.8837	4.3475	2.2267	1.6534	13.9359
PS 20 400	0.9288	0.3710	2.7627	0.2410	1.3261
	1.9062	0.7614	2.7604	0.4251	2.3391
	3.7730	1.5071	2.7484	0.7440	4.0938
	5.5871	2.2318	2.7383	1.0583	5.8233
	5.5242	2.2066	2.6981	1.0578	5.8205
	7.2429	2.8932	2.7478	1.6021	8.8155
	9.8022	3.9155	2.7120	1.7387	9.5672
	10.8923	4.3509	2.6698	1.9353	10.6489
Toluene***	0.825	0.3295	3.367	0.0480	0.1748
	0.823	0.3287	3.363	0.0437	0.1592
	2.252	0.8996	3.381	0.0754	0.2746
	3.630	1.4500	3.363	0.0697	0.2538
	4.527	1.8083	3.362	0.0829	0.3019
	6.278	2.5077	3.353	0.0882	0.3212
	8.009	3.1992	3.344	0.1018	0.3706
	8.009	3.1992	3.350	0.1096	0.3992
	10.51	4.1982	3.342	0.1272	0.4633
	12.47	4.9811	3.337	0.1393	0.5073
	12.45	4.9732	3.352	0.1570	0.5718
	12.44	4.9692	3.349	0.1530	0.5572

* Corrected for extra-column effects.

** Calculated with the average μ_1' for each solute.

*** Early-stage conditions.

Table III lists the values of φK_c and the factor $(2\varphi K_c R_0^2/15\,(1+\varphi K_c)^2)$ for the different solutes. The average μ_1' over the whole range of flow velocities for each solute was used in the underlying calculations.

TABLE III

VALUES OF φK_c AND $[2\varphi K_c/15\,(1+\varphi K_c)^2]\cdot R_0^2$ FOR DIFFERENT MOLECULES

Molecule	μ_1' *(g THF)*	μ_1' – μ_1' *(PS 411 000) (g THF)*	φK_c	$[2\varphi K_c/15\,(1+\varphi K_c)^2]\cdot R_0^{2*}$
PS 411 000	1.7107	0	0	0
PS 160 000	1.8916	0.1809	0.1057	$4.503\cdot10^{-7}$
PS 97 200	2.0322	0.3215	0.1879	$6.935\cdot10^{-7}$
PS 51 000	2.2055	0.4948	0.2892	$9.063\cdot10^{-7}$
PS 20 400	2.7297	1.0190	0.5957	$12.185\cdot10^{-7}$
Toluene	3.3553	1.6446	0.9614	$13.016\cdot10^{-7}$

* $R_0 = 0.00625$ cm.

For each molecule we shall determine the velocity of diffusion inside a pore of the column filling material, D_r, with the aid of eqn. 13. By means of non-linear regression analysis[28], it is possible to find the best fit of this equation to our experimental data. In the same procedure, values are found for A and D^1. The value of the molecular diffusion, D_m, cannot be determined in this way because the second term on the right-hand side of eqn. 13 in our experiments has a negligible value compared with the contribution of the other two terms. D_m in liquids is of the order of 10^{-5}–10^{-7}, while A is about 10^{-1}. The determination of D_m with this equation would require very unrealistic accuracies in the measurement of μ_1 and μ_2. We shall therefore omit this second term, because its retention would have an adverse effect on the determination of A, D_r and D^1.

The above does not mean that A, D_r and D^1 can each be estimated with the same accuracy in each experiment. Their relative contributions to the value of $L\cdot(\mu_2/(\mu_1')^2)$ may differ widely for each solute, and even for one substance they vary if several velocities of the mobile phase are considered.

The value of the intercept term, $2A$, is estimated most conveniently by choosing a molecule for which it makes a considerable contribution to the value of $L\cdot[\mu_2/(\mu_1')^2]$ at different velocities. With toluene this condition is fulfilled, as is apparent from a comparison of Fig. 12 with Figs. 8–11. On the other hand, it can be seen from Fig. 12 that the spread in the determination of experimental values makes it impossible to decide whether the curved function (with $D^1 \neq 0$) is a better description than the straight line (with $D^1 = 0$). Fortunately, differences in the value of A so determined amount to only 3%. The value of A found from the toluene experiments is used as a fixed value in fitting eqn. 13 with non-linear regression to the different polystyrene measurements. In consequence, two variables, A and D_m, are held constant and only the other two, D_r and D^1, are determined.

In our experiments the variance of the measured values of $L\cdot(\mu_2/(\mu_1')^2)$ increased with increasing velocities of the mobile phase, approximately in proportion to the velocity proper. Therefore, each experimental point was given a weight of $(1/u)$

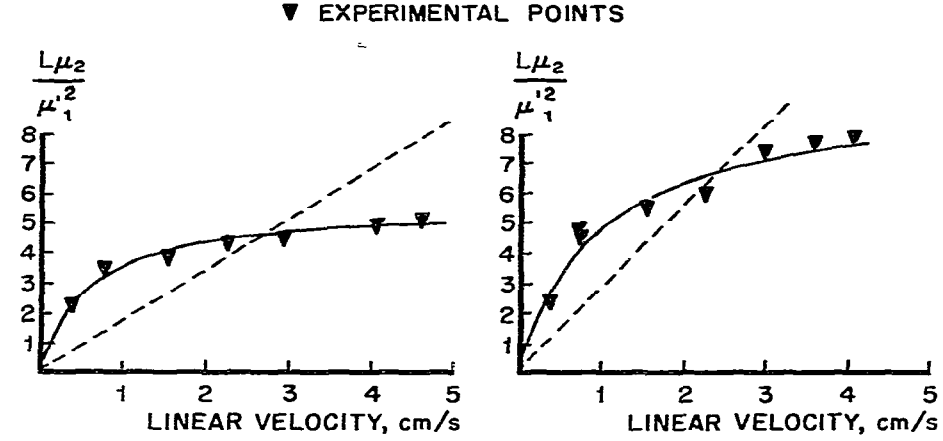

Fig. 8. Dependence of the value of $L \cdot \mu_2/(\mu_1')^2$ on flow-rate for polystyrene 160 000.
Fig. 9. Dependence of the value of $L \cdot \mu_2/(\mu_1')^2$ on flow-rate for polystyrene 97 200.

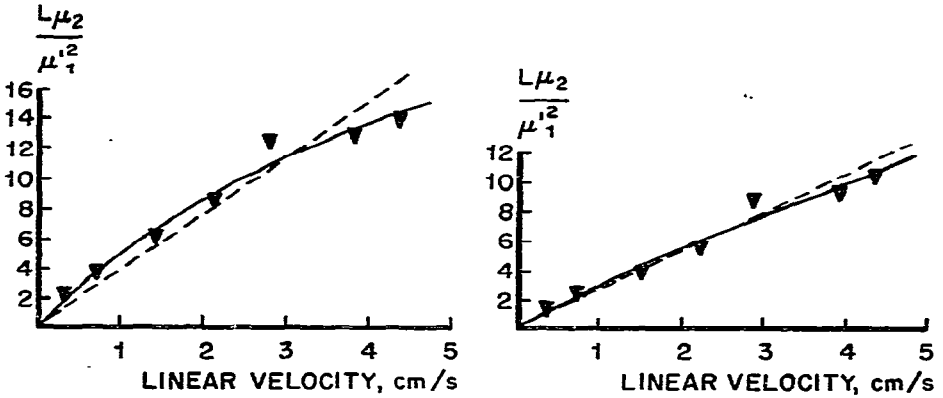

Fig. 10. Dependence of the value of $L \cdot \mu_2/(\mu_1')^2$ on flow-rate for polystyrene 51 000.
Fig. 11. Dependence of the value of $L \cdot \mu_2/(\mu_1')^2$ on flow-rate for polystyrene 20 400.

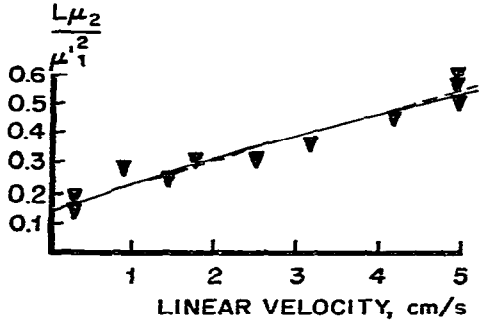

Fig. 12. Dependence of the value of $L \cdot \mu_2/(\mu_1')^2$ on flow-rate for toluene.

in the regression analysis. The results of all of the regression analyses are compiled in Table IV. The accuracy of the determination of each variable is indicated by the standard deviation, S, included in separate columns.

TABLE IV

RESULTS OF REGRESSION ANALYSIS

Molecule	A	S_A	D_m	D_r (cm^2/sec)	S_{D_r}	D^1	S_{D^1}	D_m^{LS}	D_r/D_m^{LS}
PS 160 000	0.073*	—	0*	$0.476 \cdot 10^{-7}$	$3.0 \cdot 10^{-9}$	$8.26 \cdot 10^{-8}$	$2.7 \cdot 10^{-9}$	$3.99 \cdot 10^{-7}$	0.119
PS 97 200	0.073*	—	0*	$0.731 \cdot 10^{-7}$	$5.2 \cdot 10^{-9}$	$7.40 \cdot 10^{-8}$	$3.9 \cdot 10^{-9}$	$5.43 \cdot 10^{-7}$	0.135
PS 51 000	0.073*	—	0*	$1.621 \cdot 10^{-7}$	$1.5 \cdot 10^{-8}$	$2.59 \cdot 10^{-8}$	$5.4 \cdot 10^{-9}$	$7.65 \cdot 10^{-7}$	0.212
PS 20 400	0.073*	—	0*	$4.077 \cdot 10^{-7}$	$3.5 \cdot 10^{-8}$	$2.09 \cdot 10^{-8}$	$1.1 \cdot 10^{-8}$	$12.7 \cdot 10^{-7}$	0.312
Toluene	0.073	0.005	0*	$1.66 \cdot 10^{-5}$	$1.1 \cdot 10^{-6}$	0*	—	$2.32 \cdot 10^{-8}$	0.716

* Variable is kept constant at the indicated value during regression analysis.

The values of the molecular diffusion coefficients of the polystyrenes, D_m^{LS}, in bulk THF solution were obtained by measuring the width of a scattered laser line[29,30]. Mandema and Zeldenrust[31] carried out these measurements with a home-made instrument. For toluene we estimated the molecular diffusion in THF with the method described by Scheibel[32–34]. We also applied the approximation equation of Wilke and Chang[33–35], which resulted in a value of $2.44 \cdot 10^{-5}$ cm^2/sec. Because Reid and Sherwood[34] found Scheibel's equations to yield slightly more accurate results than Wilke and Chang's method for some solvents, we entered the Scheibel value in the D_m^{LS} column of the table.

DISCUSSION AND CONCLUSION

Although the polystyrenes we used are not monodisperse, the molecular weight distribution is still very narrow. A large difference (a factor of two) in average molecular weight gives a small difference in μ_1 values, which is even much smaller than the broadening of one peak itself. Hence, for the molecules we used with $(M_w/M_n) < 1.06$, the contribution to total line broadening due to the molecular weight distribution can safely be neglected. We also assumed in our work that the contribution to the broadening that is due to the inter-particle flow effects in the column is quantitatively the same at each flow-rate for all different solutes. On this basis we assigned the same value to the factor A in eqn. 13 both for toluene and for the different polystyrenes. The extent to which this is justified was not studied in detail. However, as can be seen from Figs. 8–11, the cut-off on the $L \cdot \mu_2/(\mu_1')^2$ axis at zero velocity is very small, and also if we had chosen a different value for A in the polystyrene calculations the resulting D_r and D^1 values would hardly have been changed. The trends emerging from Figs. 8–11 were experimentally confirmed in the non-linear regression analysis, as it proved impossible to determine the value of A together with D_r and D^1 in the polystyrene experiments, *i.e.*, we found a scatter in the value of these three parameters of the same order of magnitude as or larger than the determined values of the parameters proper. Clearly, with the accuracy of our experiments, it is possible with polystyrene to determine at most two different factors separately. This is not

only a matter of accuracy but also depends on the ratio of the distinct factors with respect to each other. Exceptionally high accuracy would be required to determine a small factor together with large ones in a regression analysis. This applies even more to the determination of D_m, which is much smaller. The values of D_r resulting from our analysis seem reasonable. Measuring toluene as a control, we found a D_r value that was about 70% of the value of the D_m^{LS} in bulk solution (see Table IV). In a pore large compared with the size of a solute molecule, one would expect to obtain a D_r value similar to that of the molecular diffusion in bulk solution (probably slightly smaller), and this is the result we obtained. Thus, although we have no absolute proof, we consider that there is a sound basis for accepting the values of D_r that we found for the polystyrene molecules.

However, there is more evidence that gives confidence in the different results. We not only obtained smaller values of D_r for larger polystyrene molecules but also the D_r/D_m^{LS} ratios followed the same trend. This would be expected physically because the larger is the molecule in comparison with the pore size, the more the diffusion will be hampered by the tortuosity of the irregularly shaped pores. A theoretical description is still under investigation. Considering the evidence, we are inclined to question the assumption of Kubín[20] about the molecular weight dependence of the coefficient of diffusion in the packing, which he suggested has the same form as in bulk solution corrected by a fixed tortuosity factor of 50%.

No firm interpretation of the factor uD^1 is available. It can be attributed either to eddies or to flow through all[4] or part[7] of the pores. The broken lines in Figs. 8–12 show what happens if we neglect the factor uD^1 completely, which, of course, is identical with applying eqn. 5. It can only be concluded that next to diffusion a velocity-dependent factor must also be taken into account. In fact, we found just the opposite of the effect that is suggested by the restricted diffusion theory[8]. With increasing velocity, the mass exchange between the mobile and the stationary phase is not obstructed but is facilitated by the extra convective term.

Although eqn. 13 is mathematically equivalent to that of Giddings' coupling theory[36–38], it must be stressed that eqn. 13 describes a completely different process. The coupling theory deals with a transport process in the mobile phase outside the porous grains. If we apply the reasoning of Sie and Rijnders[39] to our solutes (with a diffusion constant of about 10^{-7} cm^2/sec), it can be seen that the coupling theory only plays a role at mobile phase velocities that are at least four orders of magnitude smaller than those which we applied in our experiments. The combination of the D_r and uD^1 terms is simply meant to describe the mass transport within the pores.

We conclude that the stationary phase part of the exchange of solutes between the two phases consists of two separate and distinguishable contributions, one due to diffusion and the other due to convection.

ACKNOWLEDGEMENTS

The authors thank Mr. M. C. C. Alta and his co-workers for the design and development of the digital data logging system and Mr. J. D. J. Grinwis for his help in the design of the appropriate software. They also owe Messrs. W. Mandema and H. Zeldenrust many thanks for the determination of the diffusion coefficients in bulk solution.

REFERENCES

1 J. Porath, *Pure Appl. Chem.*, 6 (1963) 233.
2 T. C. Laurent and J. Killander, *J. Chromatogr.*, 14 (1964) 317.
3 J. C. Giddings, E. Kučera, C. P. Russell and M. N. Meyers, *J. Phys. Chem.*, 72 (1968) 4397.
4 E. A. DiMarzio and C. M. Guttman, *J. Polym. Sci., Part B*, 7 (1969) 267.
5 E. A. DiMarzio and C. M. Guttman, *Macromolecules*, 3 (1970) 131.
6 C. M. Guttman and E. A. DiMarzio, *Macromolecules*, 3 (1970) 681.
7 F. M. Verhoff and N. D. Sylvester, *J. Macromol. Sci., Chem.*, 4 (1970) 979.
8 W. Ackers, *Biochemistry*, 3 (1964) 723.
9 W. W. Yau, C. P. Malone and H. L. Suchan, *Separ. Sci.*, 5 (1970) 259.
10 R. N. Kelley and F. W. Billmeyer, *Separ. Sci.*, 5 (1970) 291.
11 M. Kubín, in Z. Deyl, K. Macek and J. Janák (Editors), *Liquid Column Chromatography*, Elsevier, Amsterdam, 1975, Ch. 5, pp. 57–67.
12 M. Kubín, *Collect. Czech. Chem. Commun.*, 30 (1965) 1104.
13 M. Kubín, *Collect. Czech. Chem. Commun.*, 30 (1965) 2900.
14 E. Kučera, *J. Chromatogr.*, 19 (1965) 237.
15 O. Grubner, *Advan. Chromatogr.*, 6 (1968) 173.
16 S. N. Chesler and S. P. Cram, *Anal. Chem.*, 43 (1971) 1922.
17 L. Lapidus and N. R. Amundson, *J. Phys. Chem.*, 56 (1952) 984.
18 J. Crank, *The Mathematics of Diffusion*, Oxford Univ. Press, London, 1956.
19 P. R. Kasten, L. Lapidus and N. R. Amundson, *J. Phys. Chem.*, 56 (1952) 683.
20 M. Kubín, *J. Chromatogr.*, 108 (1975) 1.
21 M. E. van Kreveld and N. van den Hoed, *J. Chromatogr.*, 83 (1973) 111.
22 W. B. Innes, *Anal. Chem.*, 28 (1956) 332.
23 A. Y. Mottlau and N. E. Fisher, *Anal. Chem.*, 34 (1962) 715
24 S. T. Sie and N. van den Hoed, *J. Chromatogr. Sci.*, 7 (1969) 257.
25 A. Savitzky and M. J. E. Golay, *Anal. Chem.*, 36 (1964) 1627.
26 A. Baan, *Ph.D. Thesis*, Eindhoven, 1975.
27 S. P. Cram, S. N. Chesler and A. C. Brown, III, *J. Chromatogr.*, 126 (1976) 279.
28 N. R. Draper and H. Smith, *Applied Regression Analysis*, Wiley, New York, 1966, pp. 272ff.
29 N. C. Ford, Jr., W. Lee and F. E. Karasz, *J. Chem. Phys.*, 50 (1969) 3098.
30 D. B. Sellen, *Polymer*, 14 (1973) 359.
31 W. Mandema and H. Zeldenrust, *Polymer*, 18 (1977) 837.
32 E. G. Scheibel, *Ind. Eng. Chem.*, 46 (1954) 2007.
33 S. Bretsznajder, *Prediction of Transport and Other Physical Properties of Fluids*, Pergamon Press, Oxford, 1971.
34 R. C. Reid and T. K. Sherwood, *The Properties of Gases and Liquids*, McGraw-Hill, New York, 1966.
35 C. R. Wilke and P. Chang, *AIChE J.*, 1 (1955) 264.
36 J. C. Giddings, *Nature (London)*, 184 (1959) 357.
37 J. C. Giddings, *Anal. Chem.*, 34 (1962) 1186.
38 J. C. Giddings, *Anal. Chem.*, 35 (1963) 1338.
39 S. T. Sie and G. W. A. Rijnders, *Anal. Chim. Acta*, 38 (1967) 3.